Optical Study of the Evolution of Charge and Spin Ordering in the Manganese Perovskite $Bi_{1-x}Ca_xMnO_3$ ($x > 0.5$)

H. L. Liu,[1] S. L. Cooper,[1] and S-W. Cheong[2]
[1]*Department of Physics and Frederick Seitz Materials Research Laboratory, University of Illinois at Urbana-Champaign, Urbana, Illinois 61801*
[2]*Bell Laboratories, Lucent Technologies, Murray Hill, New Jersey 07974 and Department of Physics and Astronomy, Rutgers University, Piscataway, New Jersey 08855*
(Received 6 August 1998)

We report an optical reflectivity study of charge and spin ordering in $Bi_{1-x}Ca_xMnO_3$ ($x = 0.74$ and 0.82) single crystals. In the high temperature phase, $T > T_{co}$, which is characterized by ferromagnetic correlations, the low-energy contribution to the optical conductivity $\sigma_1(\omega)$ is dominated by small polaron dynamics. For $T_{co} > T > T_N$, the presence of both small polaron and charge-gap-like features signifies "phase separation" behavior in which domains of ferromagnetic and antiferromagnetic order coexist. Below T_N, the polaron response is completely suppressed, and a complete charge gap develops, coincident with the onset of long-range antiferromagnetic order. [S0031-9007(98)07698-4]

PACS numbers: 71.30.+h, 75.70.Pa, 78.30.–j

The diversity of electronic and magnetic properties in the perovskite manganese oxides $R_{1-x}A_xMnO_3$ (R and A being trivalent rare-earth and divalent alkaline-earth ions, respectively) has received a great deal of attention in recent years [1–3]. In the doping range $0.2 < x < 0.5$, the manganites, e.g., $La_{1-x}Ca_xMnO_3$, undergo a paramagnetic insulator to a ferromagnetic (FM) metal phase transition upon cooling and exhibit colossal magnetoresistance near the Curie temperature. These phenomena have been described within the framework of the double exchange (DE) mechanism [4] augmented by strong Jahn-Teller (JT) lattice distortions [5], although there remains some disagreement as to the significance of JT effects in these systems [6].

More recent interest has concentrated on the antiferromagnetic (AFM) insulating ground state observed in the perovskite manganites at higher doping $x \geq 0.5$, which results in part due to the long-range ordering of charges below a charge ordering temperature T_{co}. This long-range ordering of the charges was first observed in $La_{1-x}Ca_xMnO_3$ with $x \geq 0.5$ by electron diffraction and real-space images [3,7–9], which show that the doped holes tend to order in stripes along the diagonal direction of the Mn-O square lattice. Neutron diffraction measurements indicate the presence of FM correlations above T_{co} and show that AFM spin order associated with the charge ordered (CO) state develops at the Néel temperature T_N below T_{co} [10,11]. The CO behavior also manifests itself in many other experimental measurements, including in a lattice modulation of x-ray diffraction [10], a steep increase of dc resistivity [1,3], an inflection in the magnetic susceptibility [1,3], and anomalies in the sound velocity, thermopower, as well as specific heat [3]. These findings demonstrate that the CO properties of the manganites are driven by a strong coupling of charge, lattice, and spin degrees of freedom.

In this paper we describe optical spectroscopic measurements aimed at exploring the dynamic behavior of the charge and spin ordering in $Bi_{1-x}Ca_xMnO_3$ ($x = 0.74$ and 0.82), a material isostructural to $La_{1-x}Ca_xMnO_3$ with a similar phase diagram. As discussed below, these studies allow us to directly probe the influence of charge ordering on the response of the quasiparticle state and to investigate the impact of charge ordering on both the magnetic correlations and the lattice in the low temperature phase. We show that the peculiar temperature dependence of the optical conductivity $\sigma_1(\omega)$ in (Bi,Ca)MnO_3 can be divided into three regimes: (1) In the high temperature phase, $T > T_{co}$, which is dominated by FM correlations [12], the $\sigma_1(\omega)$ spectrum below 1.5 eV is characterized by a weak, overdamped Drude-like response at $\omega = 0$ eV and a broad midinfrared (MIR) absorption near 0.25 eV. These two features can be attributed, respectively, to activated $Mn^{3+} \rightarrow Mn^{4+}$ hopping and photoionization of a self-trapped carrier, i.e., a small polaron, similar to that observed in the paramagnetic response of the manganites in the low doping regime [13,14]. (2) In the intermediate temperature regime, $T_{co} > T > T_N$, the MIR band splits into two components: (i) a remnant of the small polaron contribution observed in the high temperature phase, which decreases in intensity with decreasing temperature due to the progressive freezing out of small polarons via charge ordering; and (ii) a higher-energy contribution near 0.6 eV that gradually evolves into a charge gap below T_N. The presence of these two components suggests "two-phase" behavior in this temperature range in which domains of predominantly FM and AFM spin correlations coexist. (3) For $T < T_N$, the small polaron response is completely suppressed, and the optical conductivity is characterized

 0031-9007/98/81(21)/4684(4)$15.00

by a clear charge gap and splitting of the optical Mn-O stretching mode due to long-range charge ordering.

Single-crystalline samples of $Bi_{1-x}Ca_xMnO_3$ ($x = 0.74$ and 0.82) used in the present study were grown by the flux method. The critical transition temperatures T_{co} and T_N are found to be 290, 120 K for $x = 0.74$ and 210, 160 K for $x = 0.82$, respectively [12]. The reflectance spectra at various temperatures were measured on the (001) face of the two crystals in the photon energy range (0.01–2 eV). The optical conductivity was obtained from a Kramers-Kronig (KK) analysis of the reflectance, supplemented by room-temperature ellipsometric measurements in the higher-energy region (1.5–6 eV). We found that the choice of the low-energy extrapolation does not effect the conductivity results above 0.01 eV. As a check on our KK results, the $\omega \to 0$ limit of the far-infrared optical conductivity is consistent with the measured dc conductivity in all cases (see Fig. 2) [12]. Between the highest-energy data point and 30 eV, the reflectance was merged with the data of Jung *et al.* for $La_{0.2}Ca_{0.8}MnO_3$ [15]; beyond this energy range a free-electron-like behavior of ω^{-4} was used.

Figure 1 shows (a) reflectance and (b) optical conductivity spectra for $Bi_{0.18}Ca_{0.82}MnO_3$ at several temperatures. The $x = 0.74$ sample gave qualitatively similar results. We begin by examining the room-temperature results. There are three notable features seen in the measured spectra: first, sharp phonon resonances below 0.1 eV; second, a broad absorption band at ~0.25 eV, but no pronounced Drude-like response typical of a good metal; and third, optical excitations near 3.5 and 5.3 eV that can be associated with charge-transfer transitions between O $2p$ and Mn $3d$ states [16]. Above $T_{co} \sim 210$ K, we observe only small changes in the optical response. However, upon crossing the CO transition, the optical conductivity exhibits a dramatic change as a function of temperature: the low-energy spectral weight is suppressed and transferred to energies as high as 3 eV, indicating that charge ordering causes significant changes in the electronic structure over a wide energy range. A similar temperature dependence has been observed in the optical spectra of other CO systems including pseudocubic perovskite manganite $Pr_{0.6}Ca_{0.4}MnO_3$ [17] and two-dimensional layer structure nickelate $La_{1.67}Sr_{0.33}NiO_4$ [18].

Consider first the phonon response in Fig. 2, which shows the expanded portion of the conductivity spectra

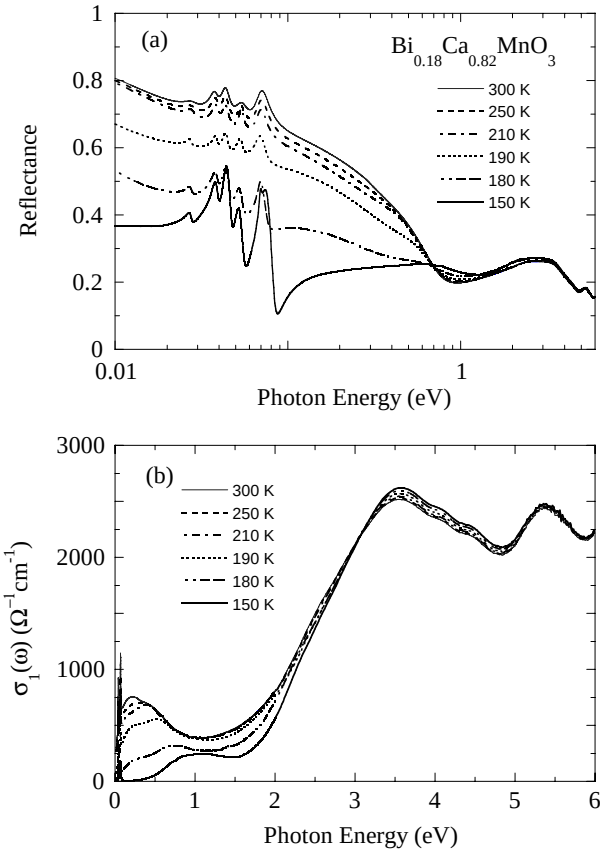

FIG. 1. (a) Reflectance and (b) optical conductivity spectra of $Bi_{0.18}Ca_{0.82}MnO_3$ below 6 eV for various temperatures.

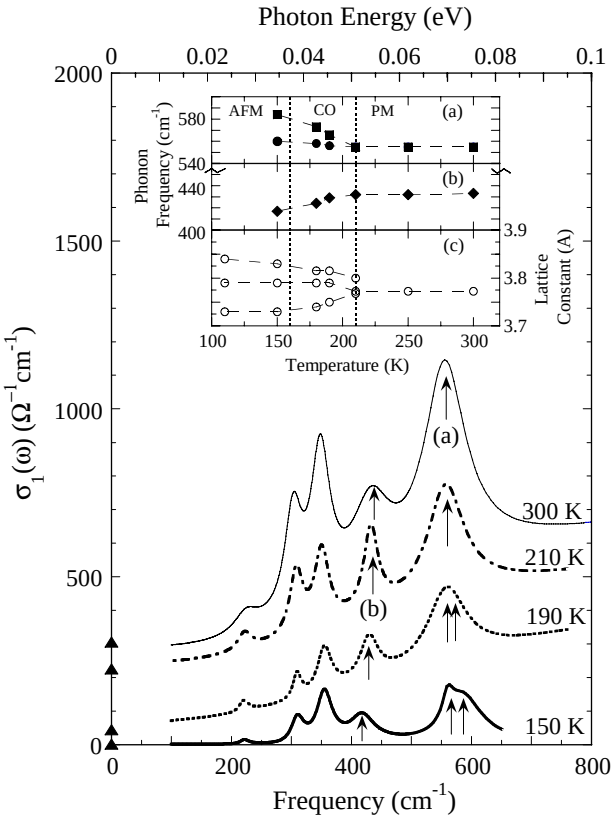

FIG. 2. Temperature dependence of optical conductivity spectra in the low-energy region (0–0.1 eV). The symbols (filled triangles) on the vertical axis represent the dc conductivity at respective temperatures [12]. The insets (a) and (b) show the phonon frequencies versus the temperatures. The inset (c) displays lattice parameters as a function of temperature [12]. AFM: antiferromagnetic; CO: charge ordered; PM: paramagnetic.

in the low-energy (0–0.1 eV) region. The 300 K $\sigma_1(\omega)$ exhibits four vibrational features on top of the electronic background. The phonon eigenfrequencies are not close to those reported for underdoped $La_{1-x}Ca_xMnO_3$ [19,20]. In particular, in (Bi,Ca)MnO_3, there is a double mode at ~307 and 347 cm^{-1} and an additional phonon peak near 436 cm^{-1}, whereas only one bending mode around 330 cm^{-1} is observed in $La_{1-x}Ca_xMnO_3$. This difference demonstrates that the replacement of La ions with smaller Bi ions causes significant changes in the environments surrounding the MnO_6 octahedra. While the frequency of the observed phonons is nearly independent of temperature above the CO temperature, there are several important changes in certain modes below T_{co}: (i) a softening of the 436 cm^{-1} Mn-O bending mode through the CO transition, which betrays some coupling of this mode to electronic degrees of freedom; and (ii) a gradual splitting of the 555 cm^{-1} Mn-O stretching mode. This behavior is consistent with electron diffraction measurements of (Bi,Ca)MnO_3, which show that the CO transition is coincident with a structural transition, as evidenced by the observation of superlattice peaks and large changes in the lattice parameters below T_{co} (see open circles in Fig. 2 [inset (c)] [12]. In particular, the splitting of the 555 cm^{-1} Mn-O stretching mode is a direct reflection of the ordering of the e_g orbitals on the Mn^{3+} sites.

As mentioned above, the most interesting changes below T_{co} occur in the electronic contribution to the optical conductivity. We analyze our results in terms of a Drude-Lorentz model and focus on the temperature behavior of the low-energy (<1 eV) spectra shown in Fig. 3. Above T_{co}, the optical conductivity in (Bi, Ca)MnO_3 can be well described by a weak, overdamped Drude contribution and a large peak (*A*) near 0.25 eV. This optical response is quite similar to that in the paramagnetic phase of the manganese perovskites for $x < 0.5$ [13,14], and can be attributed to the presence of small polarons, i.e., a small far-infrared conductivity associated with the activated hopping of small polarons, and a peak at higher energies due to photoionization of the small polarons [21]. By lowering the temperature and crossing the CO transition, the polaron response changes dramatically: (i) The far-infrared conductivity drops rapidly; and (ii) the integrated intensity of peak (*A*) decreases systematically to zero between T_{co} and T_N [see Fig. 3, inset (a)]. This behavior illustrates that charge ordering evolves as a consequence of the freezing out of small polarons. Also, as the temperature is decreased between $T_{co} > T > T_N$, an additional peak (*B*) in the conductivity develops near 0.6 eV, eventually evolving into a clean charge gap below T_N. Notably, the development of the complete charge gap at T_N coincides with the fully resolved splitting of the 555 cm^{-1} stretching mode, providing further evidence that the charge gap is associated with long-range charge ordering near T_N.

Significantly, the development of the two components (*A* and *B*) in $\sigma_1(\omega)$ at $T_{co} > T > T_N$ is consistent with neutron scattering evidence that the magnetic intensity from AFM clusters develops at the expense of magnetic intensity from FM clusters [12]. Indeed, our optical data strongly suggest that the wide temperature range between T_{co} and T_N is typified by two-phase behavior, i.e., a coexistence of charge ordering regions, perhaps in the form of stripe fragments along with regions typical of the high temperature phase in which thermally activated (ferromagnetic) $Mn^{3+} \rightarrow O \rightarrow Mn^{4+}$ hopping persists. This observation of phase separation between hole-rich FM domains and hole-poor AFM domains near the CO regime of the highly doped manganese perovskites is consistent with recent predictions [22] and demonstrates the process by which this material transitions between two distinct phase regimes while minimizing the strain energy.

The nature of the charge gap we observe in the optical conductivity, as well as its relationship to the

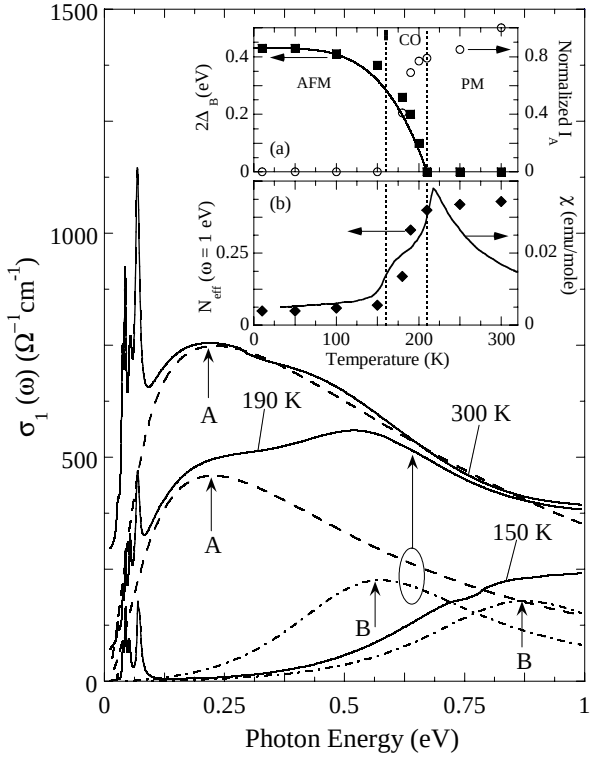

FIG. 3. The $\sigma_1(\omega)$ spectra below 1 eV at 300, 190, and 150 K. The dashed and dot-dashed lines show the fitting results by a Drude-Lorentz model (see text). The contributions of the Drude term and the high-energy (above 1 eV) interband transitions are omitted for clarity. The inset (a) shows the temperature dependence of the magnitude of the energy gap 2Δ (filled squares) and the polaron oscillator strength normalized to its 300 K value (open circles). The solid line represents the BCS function. The inset (b) shows the effective number of carriers integrated up to 1.0 eV (filled diamonds) versus the temperatures. The solid line represents the temperature dependence of the magnetic susceptibility [12]. AFM: antiferromagnetic; CO: charge ordered; PM: paramagnetic.

magnetic structure below T_N in (Bi, Ca)MnO_3, can be more carefully explored by considering the evolution of the low-energy spectral weight and the gap energy with temperature. First, Fig. 3 [inset (b)] compares the temperature dependence of the effective number of carriers per Mn atom, $N_{\text{eff}}(\omega) = (2m_0V/\pi e^2)\int_0^\omega \sigma_1(\omega')d\omega'$, integrated to 1 eV, where m_0 is taken as the free electron mass, and V is the volume containing one Mn atom, to that of the magnetic susceptibility, showing that the development of the charge gap correlates well with the onset of AFM ordering. Second, we have estimated the magnitude of the charge gap (2Δ) by linearly extrapolating the leading edge of the band (B). The resulting 2Δ versus temperature is plotted in Fig. 3 [inset (a)]. This plot shows that the energy gap is approximately zero at $T_{co} \sim 210$ K, then gradually increases with decreasing temperature to a maximum value of 0.43 eV, in a manner consistent with the (mean-field) BCS function. The fact that the temperature variation of the energy gap follows a BCS functional form suggests that it is connected with the fundamental order parameter associated with the AFM state and hence might be associated with a charge-density-wave/spin-density-wave-type gap. Indeed, very similar behavior of an opening of the charge gap has been observed in other systems with AFM ground states, such as Cr metal [23] and $NdNiO_3$ [24]. Notably, the ratio of $2\Delta(T = 0\ \text{K})/k_BT_{co}$ for both $x = 0.74$ and 0.82 samples is $\sim$18 and 24, which is significantly larger than the mean-field gap parameter value of 3.5. A large value for the gap parameter was also observed in Cr metal ($\sim$5.2) [23] and $NdNiO_3$ ($\sim$20) [24] as well as that of the CO state of $Pr_{0.6}Ca_{0.4}MnO_3$ ($\sim$9) [17] and $La_{1.67}Sr_{0.33}NiO_4$ ($\sim$13) [18] and appears to reflect the effects of strong electronic correlations.

In summary, the optical response of single-crystal $Bi_{1-x}Ca_xMnO_3$ ($x = 0.74$ and 0.82) clearly demonstrates that there exists a strong interplay between charge ordering, magnetism, and lattice coupling. At high temperatures above T_{co}, the low-energy $\sigma_1(\omega)$ exhibits Drude-like and MIR features consistent with the picture that this phase involves thermally activated hopping of self-trapped e_g electrons between Mn^{3+} and Mn^{4+} sites, resulting in FM spin correlations induced by the DE mechanism [12]. For $T_{co} > T > T_N$, the coexistence of a polaron response and a charge-gap-like structure in the optical response signifies two-phase behavior characterized by domains of both FM and AFM spin correlations. Charge ordering gives rise to a structural transition that is also observed in the softening of the Mn-O bending mode and splitting of the Mn-O stretching mode. Below T_N, our optical data exhibit a fully formed charge gap that coincides with a resolvable splitting of the Mn-O stretching mode, both indications of long-range charge ordering. The change in the low-energy optical spectral weight, N_{eff}, correlates well with the magnetic susceptibility reflecting a close correspondence of charge ordering with the development of the AFM state.

We acknowledge G. Blumberg, A. Moreo, and M. B. Salamon for helpful discussions. This work is supported by the Department of Energy under Grant No. DEFG02-96ER45439.

[1] P. Schiffer *et al.*, Phys. Rev. Lett. **75**, 3336 (1995).
[2] C. H. Chen and S-W. Cheong, Phys. Rev. Lett. **76**, 4042 (1996).
[3] A. P. Ramirez *et al.*, Phys. Rev. Lett. **76**, 3188 (1996).
[4] C. Zener, Phys. Rev. **82**, 403 (1951); P. W. Anderson and H. Hasegawa, *ibid.* **100**, 675 (1955); J. Goodenough, *ibid.* **100**, 564 (1955); P.-G. de Gennes, *ibid.* **118**, 141 (1960).
[5] A. J. Millis, P. B. Littlewood, and B. I. Shraiman, Phys. Rev. Lett. **74**, 5144 (1995); A. J. Millis, B. I. Shraiman, and R. Mueller, Phys. Rev. Lett. **77**, 175 (1996); A. J. Millis, Nature (London) **392**, 147 (1998).
[6] C. M. Varma, Phys. Rev. B **54**, 7328 (1996).
[7] C. H. Chen and S-W. Cheong, Phys. Rev. Lett. **76**, 4042 (1996).
[8] C. H. Chen and S-W. Cheong, J. Appl. Phys. **81**, 4326 (1997).
[9] S. Mori, C. H. Chen, and S-W. Cheong, Nature (London) **392**, 473 (1998).
[10] P. G. Radaelli *et al.*, Phys. Rev. B **55**, 3015 (1997).
[11] H. Kawano *et al.*, Phys. Rev. Lett. **78**, 4253 (1997).
[12] Wei Bao *et al.*, Phys. Rev. Lett. **78**, 543 (1997); Wei Bao *et al.*, Physica (Amsterdam) B (to be published).
[13] S. G. Kaplan *et al.*, Phys. Rev. Lett. **77**, 2081 (1996).
[14] M. Quijada *et al.*, http://xxx.lanl.gov/abs/cond-mat/9803201.
[15] J. H. Jung *et al.*, Phys. Rev. B **57**, R11 043 (1998).
[16] J. H. Jung *et al.*, Phys. Rev. B **55**, 15 489 (1997).
[17] Y. Okimoto *et al.*, Phys. Rev. B **57**, R9377 (1998).
[18] T. Katsufuji *et al.*, Phys. Rev. B **54**, R14 230 (1996).
[19] K. H. Kim *et al.*, Phys. Rev. Lett. **77**, 1877 (1996).
[20] Kebin Li *et al.*, J. Appl. Phys. **81**, 6943 (1997).
[21] David Emin, Adv. Phys. **24**, 305 (1975).
[22] S. Yunoki *et al.*, Phys. Rev. Lett. **80**, 845 (1998); S. Yunoki, A. Moreo, and E. Dagotto, http://xxx.lanl.gov/abs/cond-mat/9807149.
[23] A. S. Barker, Jr., B. I. Halperin, and T. M. Rice, Phys. Rev. Lett. **20**, 384 (1968).
[24] T. Katsufuji *et al.*, Phys. Rev. B **51**, 4830 (1995).